Available online at www.sciencedirect.com
SCIENCE DIRECT®
ELSEVIER
Solid-State Electronics 48 (2004) 2067–2070
SOLID-STATE ELECTRONICS
www.elsevier.com/locate/sse

Gallium-arsenide deep-level tunnel diode with record negative conductance and record peak current density

Janet L. Pan *, J.E. McManis, L. Grober, J.M. Woodall

Yale University, P.O. Box 208284, New Haven, CT 06520-8284, USA

Received 10 December 2003; accepted 15 March 2004

Abstract

Tunnel diodes utilizing deep-levels in low-temperature-grown (LTG) gallium-arsenide (GaAs) are demonstrated. These tunnel diodes achieve peak-to-valley current ratios as high as 22, a record negative-conductance-per-area of 1/226 $\Omega\,\mu m^2$, and a record peak current density of 16 kA/cm^2, all at room-temperature.
© 2004 Elsevier Ltd. All rights reserved.

PACS: 72.20.H; 73.50.F; 85.30.M; 71.55.E; 73.61.E; 85.30
Keywords: Negative resistance devices; Semiconductor defects; Semiconductor diodes; Semiconductor impurities; Tunnel diodes

1. Introduction

Tunnel diodes exhibiting negative conductance (NC) are important constituents of amplifiers and oscillators in future high-speed tetrahertz (THz) systems. The magnitude of the NC-per-area determines the maximum attainable frequency of an oscillator. Our previous work [1] was the first to show that low-temperature-grown (LTG) gallium-arsenide (GaAs) gave rise to tunnel diodes having very negative conductance and large peak current densities. In this present paper, we demonstrate tunnel diodes which utilize LTG-GaAs, and which exhibit peak-to-valley current ratios as high as 22, a record negative-conductance-per-area of 1/226 $\Omega\,\mu m^2$, and a record peak current density of 16 kA/cm^2, all at room-temperature. The previous best [2] GaAs tunnel diodes exhibited a room-temperature NC of 1/25.1 k$\Omega\,\mu m^2$ and a peak of 1.8 kA/cm^2 at a peak-to-valley current ratio of 28. These previous best [2] GaAs tunnel diodes utilized Si and Be highly doped layers at a growth temperature of 400 °C. The devices in this present paper differ from the previous ones [2] in the existence of a LTG-layer grown at 225 °C.

Our large negative conductance results from a large density of deep-states within a narrow energy range in LTG-GaAs: 10^{20} cm^{-3} of arsenic-antisite As_{Ga} [3] deep-levels. Here we will show that the peak current in the measured tunnel-diode characteristic results from transport through the deep-levels within the bandgap of the LTG region. See Fig. 2a. In contrast, the valley current in the measured tunnel-diode characteristic will be shown to result from the transport of free holes and free electrons through the valence- and conduction-bands of the LTG region, with the deep-levels acting as recombination centers (thus reducing the valley current). See Fig. 2b and c.

2. Experimental procedures

Our sample was grown in an EPI GEN II MBE system on a n-GaAs substrate. 1 μm of GaAs was grown at a pyrometer temperature of 550 °C at 1 μm/h with a Si doping of 10^{19} cm^{-3} and a As_2-to-Ga flux ratio of 15. The substrate was lowered to 225 °C during the growth of 300 nm of GaAs at 0.5 μm/h and a Si doping of

* Corresponding author.

0038-1101/$ - see front matter © 2004 Elsevier Ltd. All rights reserved.
doi:10.1016/j.sse.2004.05.071

3.5×10^{18} cm^{-3}. Then came 400 nm of LTG-GaAs at 225 °C at 0.5 μm/h and a Si doping of 3×10^{18} cm^{-3}. The substrate was raised to 350 °C during the first 100 nm of a 300 nm layer of unintentionally doped (uid) GaAs. The top layer was 200 nm of GaAs having a Be doping of 10^{20} cm^{-3} grown at 350 °C. Standard photolithography steps were used to etch mesas and deposit titanium–gold contacts. The contacts were not annealed. The p-contacts were ohmic with a resistance of 2–15 Ω. The n-contacts were weak Schottky diodes, requiring 0.6 V to reach mA currents. Radiative emission was measured with a Newport 818IG InGaAs detector.

3. Results and discussion

Fig. 1 shows measurements of four different devices on the same wafer. The device diameters, and measured room-temperature peak-to-valley current ratios, peak current densities, and negative resistances in Fig. 1a–d are, respectively, (a) 43 μm, 6.3, 1.6 kA/cm^2, 1.2 kΩ μm^2, (b) 34 μm, 8.0, 2.3 kA/cm^2, 844 Ω μm^2, (c) 34 μm, 6.5, 3.2 kA/cm^2, 795 Ω μm^2, (d) 28 μm, 22, 16 kA/cm^2, 226 Ω μm^2. The inset in Fig. 1d is an expanded view of the data in the proper part of Fig. 1d, where the points P1 and V1 denote the peak and valley currents. The NC was measured to be the slope of the straight-line connecting the points P1 and V1. The room-temperature NC of 1/226 Ω μm^2 and peak density of 16 kA/cm^2 are the largest ever in GaAs tunnel diodes. The NC-per-area determines the maximum attainable frequency [4,5] of an oscillator.

The maximum oscillating frequency [4,5] of a tunnel-diode is $|G|/(2\pi 2^{1/2}C) = t|G|/(2\pi 2^{1/2}\varepsilon A)$, where $|G|$, C, A, t, ε, are, respectively, the magnitude of the NC, the capacitance, the area, the thickness (contributing to capacitance), and dielectric constant of the device. For our best device, $A/|G| = 226\ \Omega\,\mu\text{m}^2$, $\varepsilon = 12.85$, and $t = 300$ nm contributing to capacitance, the oscillating frequency $|G|/(2\pi 2^{1/2}C)$ evaluates to be 1.3 THz. [1,2]

Significantly, radiative emission is observed only after the sharp current drops (labeled P1) in Fig. 1. This radiative emission indicates the presence of valence-band holes and conduction-band electrons. The absence of radiative emission at smaller voltages (between zero volts and the points P1 in Fig. 1) indicates a scarceness of valence-band holes and conduction-band electrons. This scarceness of free holes and electrons at smaller voltages indicates that carrier transport occurs mainly

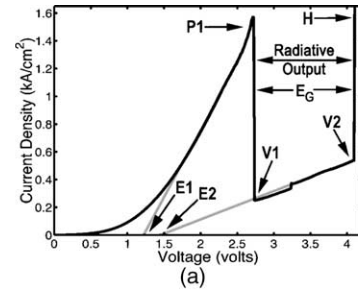

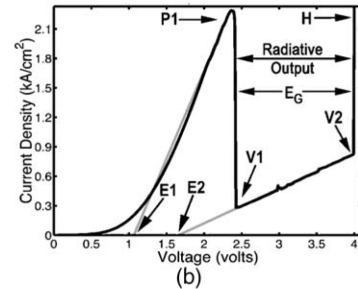

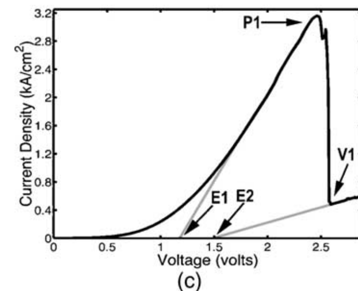

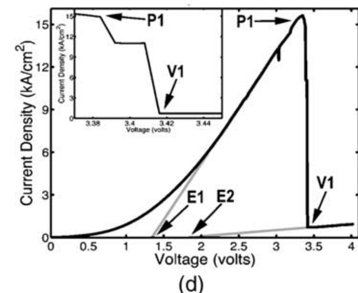

Fig. 1. Measured current–voltage characteristics of four different devices on the same wafer. The device diameters, and measured room-temperature peak-to-valley current ratios, peak current densities, and negative resistances were, respectively, (a) 43 μm, 6.3, 1.6 kA/cm^2, 1.2 kΩ μm^2, (b) 34 μm, 8.0, 2.3 kA/cm^2, 844 Ω μm^2, (c) 34 μm, 6.5, 3.2 kA/cm^2, 795 Ω μm^2, (d) 28 μm, 22, 16 kA/cm^2, 226 Ω μm^2. The inset in (d) is an expanded view of the data in the proper part of (d), where the points P1 and V1 denote the peak and valley currents. The NC was measured to be the slope of the straight-line connecting the points P1 and V1. The points E1 and E2 are extrapolations of the measured I–V curve in straight-lines to the voltage-axis. The extrapolation of the measured curve through the points V1 and V2 in a straight-line reaches the voltage-axis at the point E2. E2 is approximately one E_G.

[1] This assumes an optimal situation, in which the (positive) resistance in series with the device is $0.5/|G|$.

[2] This estimate does not include the transit time through the device.

through the deep-level E_{dl}, rather than through the conduction- and valence-bands.

In Fig. 2, the dashed lines indicate quasi-Fermi levels in the P, LTG, and N layers. Fig. 2b–d, respectively, show the energy-band diagrams in forward bias for the points V1, V2, H in the measured curves in Fig. 1a–d. Fig. 2a corresponds to the smaller voltages (between zero volts and the points P1) in Fig. 1. The positions of the quasi-Fermi levels in Fig. 2a emphasize that at these small voltages: (1) most of the applied voltage drops over the Schottky-like n-contact, and (2) carrier transport through the LTG-layer occurs mainly through E_{dl}, rather than through the conduction- and valence-bands.

The sharp drop in the total current between points P1 and V1 in Fig. 1 indicates a sharp change in the carrier transport mechanism. The relevant carrier transport mechanisms may be inferred from the shape of the measured characteristics in Fig. 1. For small voltages (between zero volts and the points P1) in Fig. 1, the measured current has the characteristic of a resistance in series with a diode of activation voltage 1–1.3 V (see extrapolation to points E1). When the total current drops (between points V1 and V2 in Fig. 1), the measured current has the characteristic of a larger resistance in series with a diode of activation voltage 1.5–1.8 V (see extrapolation to points E2). This latter activation voltage (points E2) indicates a separation in the electron and hole quasi-Fermi levels of about E_G. This quasi-Fermi level separation of E_G indicates the presence of free holes and free electrons, which is consistent with our observation of radiative emission (at both above E_G and below E_G) between points V1 and V2 in Fig. 1. This quasi-Fermi level separation characterizes the band diagrams in the LTG-layer in Fig. 2b and c, which we infer from our observations.

The large resistance measured between points V1 and V2 in Fig. 1 is a result of the small concentrations and mobilities of free carriers in the LTG-layer in Fig. 2b and c. Moreover, since E_{dl} in the LTG-layer in Fig. 2b and c does not line up with either the conduction- or valence-band of the adjacent P- or N-layer, then the free carriers which are captured into the deep-level E_{dl} must be re-emitted by E_{dl} into the conduction- or valence-bands before the free carriers can reach the opposite electrical contact. (Carrier emission out of deep-levels is slow, as required by the detailed-balance principle.) The sharp rise in the total current between points V2 and H in Fig. 1 also indicates a sharp change in both the energy-band lineup and the carrier transport mechanisms. Note that the voltage at the points V2 and H in Fig. 1 is 3 V (about $2E_G$) higher than the voltage V_F at the point E1, which is the extrapolated value of the contact voltage drop. Although the total voltage across the device is the same ($2E_G$ plus the contact drop qV_F) in Fig. 2c and d (points V2 and H in Fig. 1), in Fig. 2c, a voltage of $2E_G/q$ drops evenly through the entire LTG-layer. In contrast, in Fig. 2d, a voltage of E_G/q drops over both the P–LTG junction and the LTG–N junction, but almost no voltage drops over the LTG region. Significantly, the deep-level E_{dl} in the LTG-layer in Fig. 2d does indeed line up with the conduction- or valence-band of the adjacent P- or N-layer, in contrast to the band diagram of Fig. 2c. This provides an additional, more efficient carrier transport mechanism through the LTG-layer in Fig. 2d: that of transport through E_{dl}. As expected, the total current is then higher for the energy-band lineups in Fig. 2a and d, which are characterized by transport through E_{dl}, than for the band lineups in Fig. 2b and c (cf. points P1, H versus points V1, V2 in Fig. 1).

Device performance varied across the wafer. Devices near the edge of the wafer showed lower peak-to-valley current ratios, and lower NC. We believe this to be a result of the quality of the layer grown at 350 °C. In order to increase the peak current, this layer needs to have a large concentration of deep-states (through which transport takes place). In order to lower the valley current, this layer must also show a high enough resistance for enough voltage to drop across it, so that the deep-state energy is separated from the quasi-Fermi levels of the adjacent P and N regions. See Fig. 2b and c. The valley current will be high, if there is insufficient voltage drop across the LTG-layer, as shown in Fig. 2d.

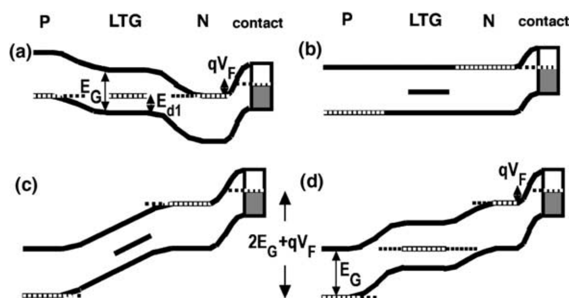

Fig. 2. Energy-band diagrams in forward bias. (a) Band-diagram corresponding to the smaller voltages (between zero volts and the points P1) in Fig. 1. The band-diagram shows that transport occurs mainly through E_{dl}. No optical emission is observed at these voltages. V_F is the voltage drop at the contact. At these voltages, significant resistance is observed in the I–V curve. This is mostly likely the resistance of the LTG region. (b) Band-diagram corresponding to the points V1 in Fig. 1. (c) Band-diagram corresponding to the points V2 in Fig. 1. In (b) and (c), significant transport occurs through the conduction- and the valence-bands. At voltages between points V1 and V2 in Fig. 1, optical emission is observed. The large resistance in the I–V curve at voltages between points V1 and V2 in Fig. 1 corresponds to the large resistance of the LTG region. (d) Band-diagram corresponding to the points H in Fig. 1. At this voltage, significant transport occurs through E_{dl}. In (d), a voltage of E_G/q drops over both the P–LTG junction and the LTG–N junction, but almost no voltage drops over the LTG region.

4. Conclusions

Tunnel diodes utilizing deep-levels in LTG-GaAs are demonstrated. These tunnel diodes achieve peak-to-valley current ratios as high as 22, a record negative-conductance-per-area of 1/226 $\Omega\,\mu m^2$, and a record peak current density of 16 kA/cm^2, all at room-temperature. Our physical model shows that the peak current results from transport through the deep-levels within the bandgap of the LTG region. Our model also shows that the valley current results from the transport of free holes and free electrons through the valence- and conduction-bands of the LTG region, with the deep-levels acting as recombination centers (thus reducing the valley current).

Acknowledgements

JLP was supported by NSF CAREER.

References

[1] Pan JL, McManis JE, Grober L, Woodall JM. Gallium arsenide deep level p-i-n tunnel diode with very negative conductance. Electron Lett 2003;39:1411–2.

[2] Ahmed S, Melloch MR, Harmon ES, McInturff DT, Woodall JM. Use of nonstoichiometry to form GaAs tunnel junctions. Appl Phys Lett 1997;71:3667–9.

[3] Melloch MR, Nolte DD, Woodall JM, Chang JCP, Janes DB, Harmon ES. Molecular beam epitaxy of nonstoichiometric semiconductors and multiphase material systems. Crit Rev Solid State Mater Sci 1996;21:189–263.

[4] Brown ER, Parker CD, Sollner TCLG. Effect of quasi-bound-state lifetime on the oscillation power of resonant tunneling diodes. Appl Phys Lett 1989;54:934–6.

[5] Sollner TCLG, Brown ER, Goodhue WD, Le HQ. Observation of millimeter-wave oscillations from resonant tunneling diodes and some theoretical considerations of ultimate frequency limits. Appl Phys Lett 1987;50:332–4.